CSCE Annual Conference

*Growing with youth – Croître avec les jeunes*

Laval (Greater Montreal)

June 12 - 15, 2019

# FINITE ELEMENT ANALYSIS OF UHP-FRC SUBJECTED TO BLAST LOADING

Sherif, M.[1,4], Othman, H.[2], Marzouk, H.[3]
[1,2,3] Ryerson University, Canada
[4] Mohtady.Sherif@Ryerson.ca

**Abstract:** Several investigations have shown that the mechanical properties of ultra-high-performance fibre reinforced concrete (UHP-FRC) material are different from traditional concrete. The differences in material behavior might result in more complexity to the finite element method (FEM) simulation of UHP-FRC under extreme loading conditions (e.g., impact, blast). This paper presents a numerical investigation on the performance of reinforced UHP-FRC panels under blast loading with a concrete material model which considers the contribution of tensile hardening response. The fracture energy of this material is about a hundred times that of normal strength. This material has 2% of steel fiber that provides an extended crack-band width that accurately represents the tensile behaviour. The concrete damage plasticity (CDP) constants were calibrated at Ryerson by two series of experimental testing. The performance of the numerical models is verified by comparing numerical results to the experimental data. A brief description of the experiment required for the validation is provided. Each input parameter of UHP-FRC is investigated to establish a precise numerical method for blast analysis and identify the significance of various effects on the numerical results. The numerical simulation has been performed using ABAQUS/Explicit. Adjust paragraph spacing like this

Experimental blast loading results reported from Korea by (Yi et al. 2012), has been used to further adjust the calibrated model, that was used to investigate the effect of steel reinforcement and the concrete thickness in increasing UHP-FRC resistance to blast loading. The numerical results demonstrate the feasibility of using calibrated CDP constitutive concrete model for analyzing UHP-FRC under high dynamic loading rates. Computed responses are sensitive to parameters related to the tension, fracture energy, strain rate effect, plastic expansion, and damage parameters.

## 1 INTRODUCTION

UHP-FRC is a special type of concrete where coarse aggregate is eliminated completely, and only fine particles are used, with an optimized grain size distribution, often referred to as particle packing, to densify the mix, enhance impermeability and high strength and improve rheology. Moreover, a superplasticizer or high range water reducer is typically used to improve rheology while maintaining the W/C as low as 0.2. Fibres usually steel or synthetic fibres should be added as a volumetric ratio up to 2% to improve ductility and achieve higher tensile and flexural strength, as well as higher fracture energy. Having an outstanding fresh and hardened properties, this includes the ease of placement and consolidation with ultra-high early and long term mechanical properties, as well as toughness volume stability, durability, higher flexural and tensile strength, fracture energy and ductility (Kosmata et al. , 2003; Graybeal, 2006; Naaman, 2007; Wille and Naaman, 2010). The research demand for the special applications of the UHP-FRC is growing higher, the material behaviour, characteristics are getting more understood as more research is being focused on it. UHP-FRC material offers a higher potential for outstanding performance in a variety of special applications, mostly limited to applications in the construction of bridges and limited applications for high rise buildings, marine, and offshore structures.

Recently, UHP-FRC is thought to have an outstanding performance in the field of defensive structures, and protective shields, specifically against blast loads (Mao et al. or 2013; Slotz et al. 2014; Rebentrost and white 2011; Cavill, Rebentrost, and ; E). The high-energy absorption capacity of UHP-FRC enables the construction of shield plates that play an important part in protecting existing strategic buildings against extreme loading conditions caused by blast, shock or impact loads ( Othman and Marzouk, 2016; Lee, Choi and ; Rebentrost and white, 2011;Schleyer et al. , 2010) Moreover, a strong engineering evidence at low speed impact tests done by (Othman and Marzouk 2016) on UHP-FRC slabs showed that UHP-FRC has more ductility and energy absorption due to the presence of fibres that bridges the cracks and thus also produces a more ductile failure mode and fewer fragmentations, than the panels of the same size and geometry made from HSC and NSC. It has been found out experimentally at Ryerson University, using fiber optic sensor of the fiber brag grating (FBG) type, that the fracture energy of UHP-FRC is about 100 times that of normal concrete (Wahba and Marzouk 2012).

On the material behaviour level, the research demand on UHP-FRC is growing higher, the material behaviour and response and how to identify it and capture the actual behaviour as well as the fracture behaviour are of specific interest to researchers over the last decade. Over the last decade, the German and Japanese codes have started to add new sections to address the different mechanical properties and limitations of this new material.

UHP-FRC is still relatively expensive material, thus, it is anticipated that UHP-FRC will find an increasing market as a thin protective cover for reinforced concrete structures in specific zones where the superior properties are needed (Habel and Gauvreau 2008).

The numerical simulation has been performed using the finite element software package ABAQUS/Explicit (Simula 2016), with a concrete material model which considers the contribution of tensile hardening response, fracture energy and crack-band width approaches to accurately represent the tensile behaviour and guarantee mesh independence of results. The complete behaviour of UHPFRC is defined using the concrete damage plasticity model. The blast load is applied using the Conventional Weapons (ConWep) method of the US Army Corps of Engineers (USACE, 2017) that is built into the finite element software (Simula 2016). The validity of the numerical model used is verified for low-speed impact against experimental test data (Othman and Marzouk 2018), and for blast loading by comparing numerical results to the available experimental data from research conducted by (Yi et al. 2012).

## 2 UHP-FRC Material

UHP-FRC has outstanding properties compared normal strength concrete NSC, high strength concrete HSC and fibre reinforced concrete FRC, in terms of workability, durability, strength. These properties are designed for by the selection and optimization of the constituents as well as the optimization of the grain size distribution and the use of an advanced super-plasticizer.

### 2.1 UHP-FRC Tensile behaviour

From the strength of materials perspective, UHP-FRC could be defined as a class of FRC composite, that exhibits a strain hardening behavior under tensile load during the first cracking and the development of the multiple cracking, till the peak tensile strength is reached, after which the material will experience stress and crack localization, and will experience strain softening, at which the strain description of the behaviour is not valid and the crack opening displacement COD is more representative ( Dobrusky and Bernardi, 2017; Wille and Naaman, 2010; Naaman 2007) as illustrated by Figure 1 and Figure 2. This behaviour is different from strain softening behaviour exhibited by other FRC composites, where they exhibit linear stress, strain relationship in the elastic stage, then suddenly it would experience stress localization and crack localization, and the curve descends immediately as illustrated in Figure 1 (Naaman 2007).

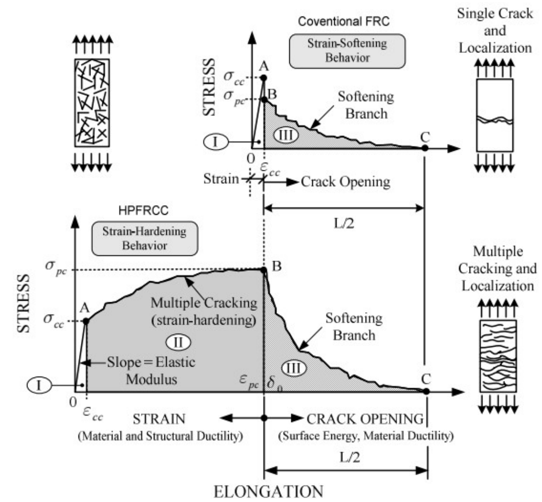


Figure 1 Stress-strain diagram illustrating strain hardening and strain softening of FRC composites. (Naaman 2007)

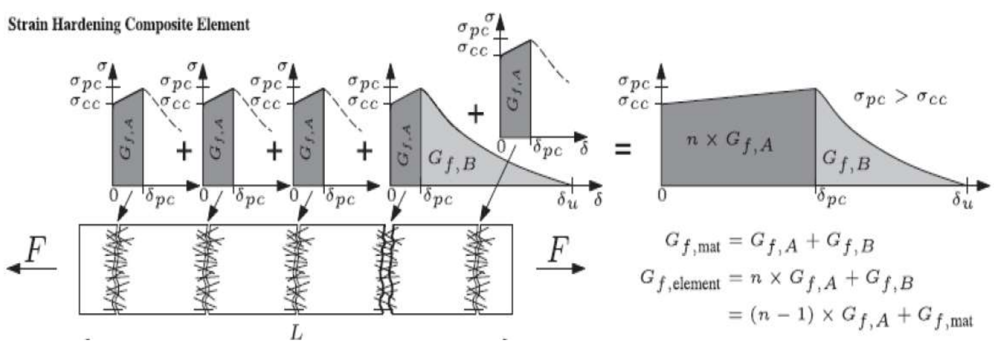


Figure 2 COD description of the material. (Xu and Wille 2015)

### 2.2 Fracture Energy of UHP-FRC concrete

The fracture behaviour and mechanics of UHP-FRC could be obtained experimentally by testing the material under direct tension, the post-cracking COD should be obtained, this could be achieved by accounting for the average crack spacing. A full COD description now could be obtained, by combining the COD measurements for each phase, as illustrated in Figure 2, and thus the fracture energy of the material could then be accurately calculated (Wille and Naaman 2010). In literature, UHP-FRC of 140–180 MPa containing 2.0% short steel fibre by volume and cured under standard conditions, showed tensile fracture energies ranging from 14,000 to 21,000 N/m (Wille and Naaman, 2010). It has been found out experimentally at Ryerson University that the fracture energy of UHP-FRC is about 100 times that of normal concrete (Wahba and Marzouk 2012).

### 2.3 UHP-FRC compressive behaviour

The compressive behaviour of UHP-FRC is characterized by the high peak strength, and by the post-peak ductility, while the latter is dedicated to the presence of steel fibres and influenced by the fibre volumetric ratio (Naaman, 2007; Othman, 2016). It is worth mentioning that although the steel fibres enhance the post-peak ductility, they do not contribute to the elastic modulus nor to the compressive strength (Naaman, 2007; Othman, 2016). Figure *4* shows a comparison between the compressive strength and response of a UHP-FRC specimen to that of an HSC Specimen tested by( Othman and Marzouk 2016, Yazidizadeh 2014) using fibre Bragg grating sensor to record all the strains, as depicted by Figure *3*. The UHP-FRC exhibited highly ductile response under compression and reached 2.7 times the strain reached by HSC at failure.

## 2.4 Flexural and bending behaviour

(Yazidizadeh 2014) at Ryerson conducted experimental using fibre optics sensor of the (FBG) type on a 160 MPa compressive strength UHP-FRC and 80 MPa compressive strength of high strength concrete (HSC). Three-point flexural strength and fracture energy tests are conducted on 100×100×400mm prisms with a clear span of 300 mm. A hydraulic servo-controlled (MTS 793) testing machine is used to perform tests for the three lower strain rates of flexural tests. The flexural strength of HSC was 7.5 MPa, while the UHP-FRC showed to be 2.7 times stronger in flexure than HSC and exhibited a more ductile response, moreover, experienced a post-peak strain softening behaviour as shown in *Figure 5* reaching a flexural strength of 20MPa.

Figure 3 Compressive Strength and Modulus of elasticity test with embedded FBG sensor (Yazidizadeh 2014).

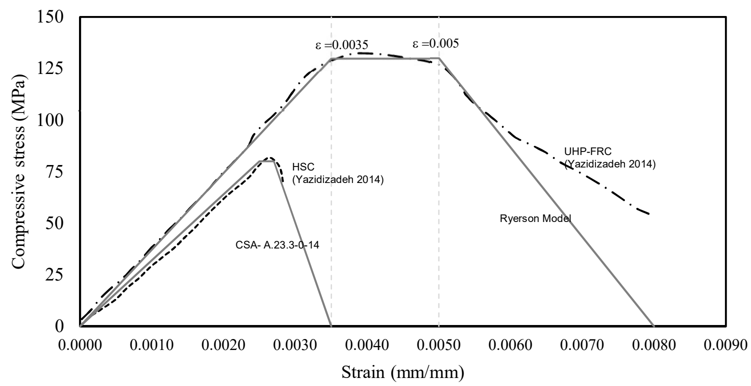


Figure 4 compressive strength of UHP-FRC and the effect of fibre volumetric ratio on the post-peak ductility.

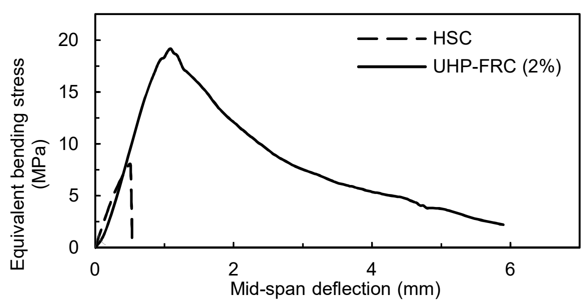


Figure 5 Flexural strength for NSC and UHP-FRC (Othman and Marzouk 2016)UHP-FRC constitutive models

Other models for the behaviour of UHP-FRC became available, some of these models are presented by the Japan Society of Civil Engineers (JSCE), and the French Association of Civil Engineering (AFGC), both models showed good results when compared to experimental results as tested by (Yoo, Banthia, and Yoon 2016). In addition, the models presented by (Gowripalan and Gilbert 2000) for compression and tension was adopted by the Australian code.

# 3 Constitutive Material Model for UHP-FRC

Any of the pre-mentioned models can be used as an input constitutive model in the finite element software, another approach is by obtaining the properties of the UHP-FRC experimentally and generating a best fit approximate plot and use it as a material input. *Figure 6* presents the material model and damage parameters used in this study.

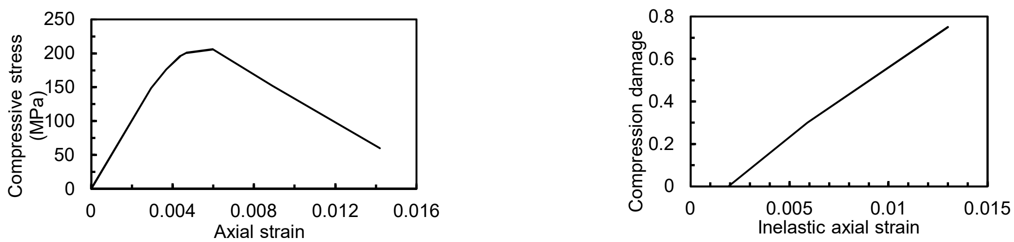


(a) Uniaxial compression parameters (left: stress-strain; right: damage)

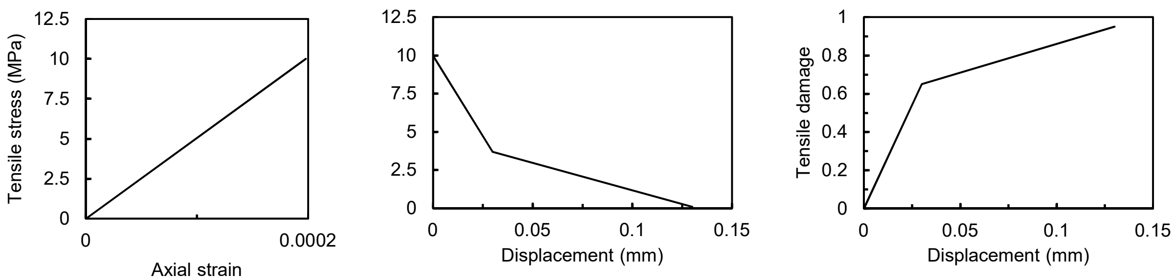


(b) Uniaxial tensile parameters (left: stress-strain/crack width; right: damage)

Figure 6 Adapted UHP-FRC uniaxial relationships for concrete damage plasticity model.

# 4 Calibration of UHP-FRC Constitutive Model

A reliable numerical model was created for UHP-FRC using and adjusted and calibrated CDP model the calibration process passed through different stages, to verify the validity and applicability of CDP modelling at higher strain rate loading.

## 4.1. Prisms Drop Hamer Testing

The UHP-FRC model was first calibrated for low-speed impact on beams tested by (Aghajani-namin 2014) at Ryerson University Figure 7 (a). Higher dynamic strain rates corresponding to impact loading have been conducted using a drop-hammer setup Figure 7. A flat-face drop hammer with a mass of 37.5 kg is released from three different heights 150, 300, 600 mm to strike the mid-span of prisms, the experimental results were then used to calibrate the CDP Numerical model. Flat-face drop hammer with a mass of 37.5 kg is released from three different heights 150, 300, 600 mm to strike the mid-span of prisms. The flexural loads and loading rates are calculated based on the total reaction time history. The reaction forces between the support and the specimens are measured using quartz cells. The raw data are sampled with a rate of 5 kHz using a digital dynamic data acquisition system. Further details about the test procedures and the calibration could be found elsewhere,  (Othman and Marzouk 2017).

## 4.2. Slab Plate Drop Hamer Testing

Further calibration of the CDP for low-speed impact on slabs by (Othman and Marzouk 2017) Figure 7 (b). Five UHP-FRC plates were constructed and tested in the Structural Laboratory of Ryerson University. All plate specimens 1950 by 1950 mm doubly reinforced with 10M bars with a thickness of 100 mm and 15 mm clear cover to reinforcement. Specimens are subjected to multi-impact tests by dropping a steel mass of 475 kg from a clear height of 4.15 m. The striking surface of the drop-weight is flat with dimensions of 400×400 mm. Specimens are subjected to impact at the midpoint and supported at the four corners. FEM model was created using ABAQUS/Explicit, the exact loading and boundary conditions were modelled in the model, a sensitivity analysis was performed, and the model was calibrated against the experimental results and it the model results were within an acceptable range from the experimental. Further details about the test procedures and the calibration could be found elsewhere,  (Othman 2016).

(a) Beams (Aghajani-namin 2014)

(b) Slabs (Othman and Marzouk 2017)

Figure 7 Material drop-hammer test setup

### 4.3. Blast Plate testing Calibration

The experimental blast test used for calibration was carried out by (Yi, et al. 2012), the model and the experimental sample were a 1000 x 1000 x 150 mm UHP-FRC slab of 210 MPa compressive strength and Young's modulus of 50 000 MPa. The slab was loaded with an equivalent charge of 15 kg of TNT at a standoff distance of 1.5m. The load was applied in ABAQUS/Explicit using the built-in what is known as (ConWep) module, the same load and standoff distance was modelled in the software. It can be observed that the mid-point displacement and pressure for the FEM model fall within an acceptable range from the experimental results. The results of the calibration for UHP-FRC are shown in Figure 11 and Figure 12.

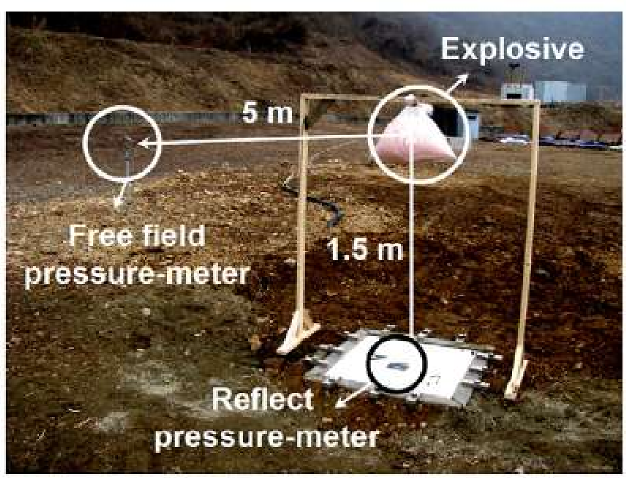


Figure 8 Test setup for the blast loading by *(Yi, et al., 2012)*

## 5 Recommended damage plasticity Model

The concrete damage plasticity model presented in ABAQUS software and most widely used in modelling concrete is a modified Drucker-Prager Yield model. In the deviatoric plane Figure 9 the concrete damage plasticity model doesn't follow a circular shape but rather is modified by a shape parameter $K_c$, which is a ratio of the second stress invariant for tension and compression at the same hydrostatic stress. For the concrete damage plasticity model, the default value of $K_c$ is 2/3 compared to $K_c$ of 1 for Drucker-Prager of normal strength concrete. The calibration of UHP-FRC model under blast load was then performed such that only the values for material parameters with a significant effect where considered, based on a sensitivity analysis conducted by (Othman and Marzouk 2017) these parameters included fracture energy (GF), uniaxial tensile strength ($f_t$) and dilation angle (ψ) as shown in. Other CDP parameters with marginal effect, including ϵ, $\sigma_{bo}/\sigma_{co}$, and $K_c$, is set to the default values of 0. 1, 1. 16, and 0. 67, respectively.

Table 1 Sensitivity analysis results (Othman and Marzouk 2017).

| Material parameter | Significance | Material parameter | Significance |
|---|---|---|---|
| Tensile strength ($f_t$) | ✓ | Flow eccentricity (ε) | × |
| Fracture energy ($G_f$) | ✓ | Shape parameters ($K_c$) | × |
| Dilation angle (ψ) | ✓ | Ratio ($\sigma_{bo}/\sigma_{co}$) | × |
| Poisson ratio (υ) | × | Damage ($d_c$,$d_t$) | ✓ |

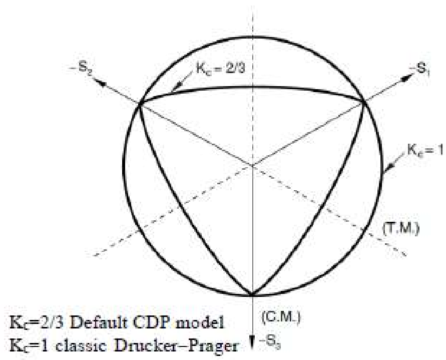


Figure 9 Concrete damage plasticity and Drucker-Prager in the deviatoric plane. (Simulia 2016)

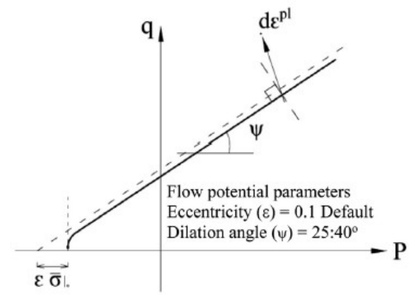


Figure 10 the meridian plane of the concrete damage plasticity model. (Simulia 2016)

It was observed in the calibration process, that the influences of material parameters on the impact force and reaction results are generally limited. Therefore, only the results of midpoint displacement, midpoint pressure and acceleration were considered (Othman and Marzouk 2014). The exact experimental test setup and loading and boundary conditions were modelled in the ABAQUS FEM for UHP-FRC.

In the meridian plane Figure 10 the concrete damage plasticity model follows the hyperbolic plastic flow potential function that is defined by the flow potential eccentricity ϵ which describes the rate by which the plastic flow function approaches asymptote, and the dilatation angle ψ, which is somehow equivalent to the concrete internal friction angle, in addition to the parameter $\sigma_{bo}/\sigma_{co}$, which is the ratio of the strength in the biaxial state to the strength in the uniaxial state. (Simulia 2016)

## 6 Numerical Analysis based on the calibrated model

The model verification results for UHP-FRC are shown in Figures 11-13. The calibrated model was used to conduct a numerical parametric study to investigate the effect of reinforcement ratio as well as the aspect ratio of wall panels of or 150 mm thickness, the slabs were constructed of an aspect ratio (length/width) of 1, 1.25, 1.5, and 1.75 and for each aspect ratio, three

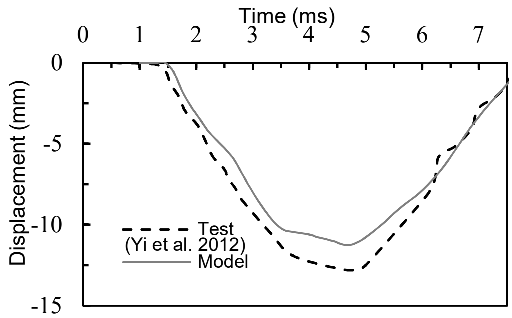


Figure 11 Mid-point displacement for UHP-FRC slab.

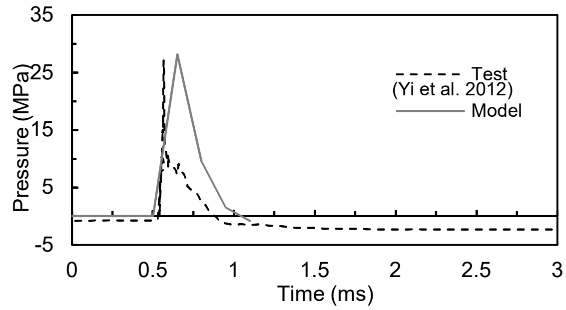


Figure 12 Mid-point incident pressure on the top surface of the UHP-FRC slab.

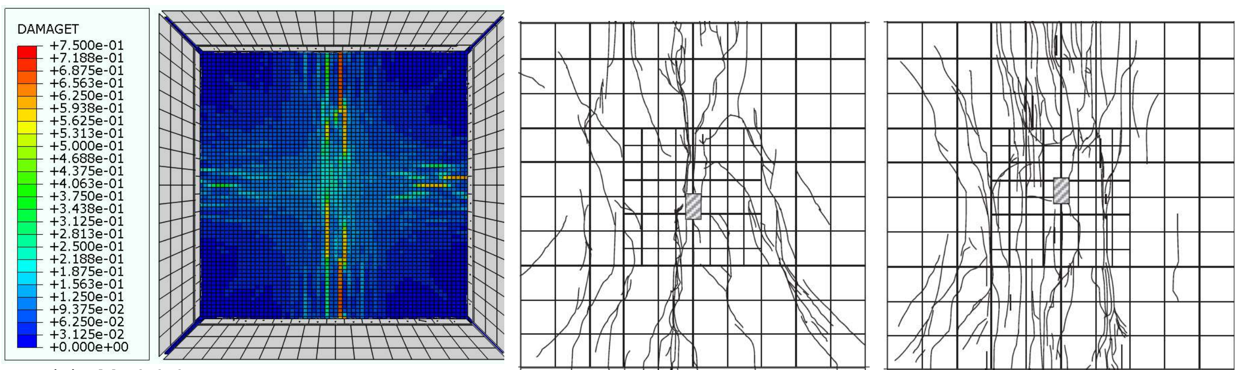


(a) Model damage pattern.

(b) Plot of the crack pattern observed in the test for UHP-FRC slab RPC1. (Yi et al. 2012)

(c) Plot of the crack pattern observed in the test for UHP-FRC slab RPC2. (Yi et al. 2012)

Figure 13 Damage and crack pattern for the UHP-FRC slab.

slabs of reinforcement ratios (ρ) of 0.00%, 0.2%, and 1%. were considered. The slabs were loaded with a load that simulates an unconfined blast load due to a truck loaded with 420 kg charge mass of TNT at standoff distances 6 m, from a protective panel this load, and distance combination gives a scaled distance of Z=0.8 m/kg$^{1/3}$. The load was simulated using the ABAQUS/Explicit built-in ConWep module.

## 7 Conclusions

The results of the parametric study were summarized in Figure *14* and Figure *15* and revealed that the reinforcement has a limited effect in improving the displacement, thus a minimum reinforcement ratio of 0.2% should be sufficient. Furthermore, from the current investigation, the following conclusions can be highlighted:

1. The concrete damage plasticity model can be used to model UHP-FRC under blast loads successfully.
2. The plastic volume change of (dilation angle) of UHP-FRC equal to 10$^{o}$ and that is small in comparison to HSC material with dilation angle equal to 40$^{o}$.
3. UHP-FRC is a promising material in the field of protective blast load structures.
4. Under blast loading, the UHP-FRC slabs exhibited a highly ductile repose, and a considerably large deflection without fragmentation and spalling before or during fracture.

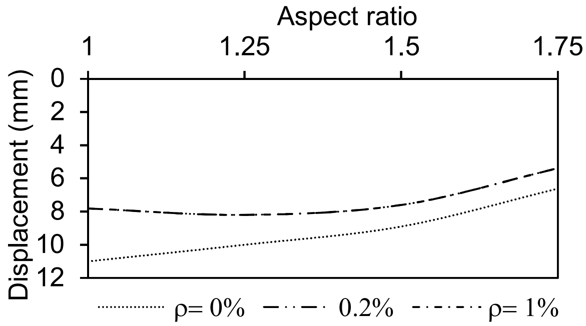


Figure 14 The aspect ratio versus maximum displacement for a slab thickness of 175mm at different reinforcement ratios.

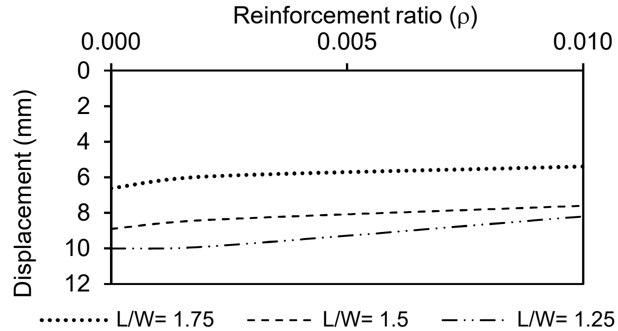


Figure 15 The reinforcement ratio versus maximum displacement for a slab thickness of 175 mm at different aspect ratios.

## 7 References

Aghajani-namin, Aria. 2014. "Strain Rate Sensitivity of UHP-FRC." M.Eng. Report, Ryerson University.

Cavill, B, M Rebentrost, and V Perry. 2006. "'Ductal®: An Ultra-High Performance Material for Resistance to Blasts and Impacts.'" In *1st Specialty Conference on Disaster Mitigation (CSCE)*, 1–10. Calgary, Canada.

Dobrusky, Svatopluk, and Sebastien Bernardi. 2017. "Uni-Axil Tensile Test for UHPFRC." In *Symposium on Ultra-High Performance Fiber Reinforced Concrete*, 165–74. Montpellier, France: AFGC-ACI-fib-RILEM Int.

Ellis, B D, B P Dipaolo, D L McDowell, and M Zhou. 2014. "Experimenta and Numerical Investigation and Multiscale Modeling of Ultra-High-Performance Concrete Panels Subject to Blast Loading." *The International Journal of Impact Engineering*, no. 69: 95–103.

Gowripalan, N, and R I Gilbert. 2000. "DEsign Guidelines for Ductal Prestressed Concrete Beams." VSL Austrailia.

Graybeal. 2006. "Material Property Characterization of Ultra-High Performance Concrete." Federal Highway Administration. Report No. FHWA-HRT-06-103.

Habel, Katrin, and Paul Gauvreau. 2008. "Response of Ultra-High Performance Fiber Reinforced Concrete (UHPFRC) to Impact and Static Loading." *Cement and Concrete Composites* 30 (10): 938–46.

Kosmata, S, B Kerkhoff, R Hooton, and R McGarth. 2003. *Design and Control of Concrete Mixture*. Cement association of Canada,.

Lee, Sang Won, Seung Jai Choi, and Jang-Ho Jay Kim. 2016. "Analytical Assessment of Blast Damage of 270,000-KL LNG Storage Outer Tank According to Explosive Charges." *Computers and Concrete* 17 (2): 201–14.

Li, Jun, Chengquing Wu, and Hong Hao. 2015. "An Experimental and Numerical Study of UHPFRC Slabs under Blast Loads." *Materials and Design 82*, 64–75.

Mao, L, S J Barnett, A Tyas, J warren, and S S Zaini. 2015. "Response of Small Scale Ultra High Performance Fibre Reinforced Concrete Slabs to Blast Loading." *Construction and Building Materials 93*, 822–30.

Millard, S, T Molyneaux, S Barnett, and X Gao. 2010. "Dynamic Enhancement of Blast-Resistant Ultra High Performance Fibre-Reinforced Concrete under Flexural and Shear Loading." *International Journal of Impact Engineering* 37 (4): 405–13.

Naaman, A. 2007. "High Performance Fiber Reinforced Cement Composites: Classification and

Applications." In *CBM-CI International Workshop*, 389–401. Karachi, Pakistan.

Ngo, Tuan, Priyan Mendis, and Ted Krauthammer. 2007. "Behavior of Ultrahigh-Strength Prestressed Concrete Panels Subjected to Blast Loading." *Journal of Structural Engineering* 133 (11): 1582–90. https://doi.org/10.1061/(ASCE)0733-9445(2007)133:11(1582).

Othman, H., and H. Marzouk. 2016. "Impact Response of Ultra-High-Performance Reinforced Concrete Plates." *ACI Structural Journal* 113: 1–10. https://doi.org/10.14359/51689157.

Othman, H, and H Marzouk. 2014. "Numerical Investigation of Reinforced Concrete Slabs under Impact Loading." In *10th Fib International PhD Symposium in Civil Engineering*, edited by Josée Bastien, Nicolas Rouleau, Mathieu Fiset, and Mathieu Thomassin, 263–70. Québec, Canada,.

Othman, Hesham. 2016a. "Performance of UHPFRC Plates under Impact Loads." *PhD. Dissertation*. Toronto: Ph.D. dissertation, Ryerson University.

Othman, Hesham, and Hesham Marzouk. 2017. "Finite-Element Analysis of Reinforced Concrete Plates Subjected to Repeated Impact Loads" 143 (9): 1–16. https://doi.org/10.1061/(ASCE)ST.1943-541X.0001852.

Othman, Hesham, and Hesham Marzouk. 2018. "Applicability of Damage Plasticity Constitutive Model for Ultra-High Performance Fibre-Reinforced Concrete under Impact Loads." *International Journal of Impact Engineering* 114 (August 2017): 20–31. https://doi.org/10.1016/j.ijimpeng.2017.12.013.

Rebentrost, M, and G white. 2011. "Investigation of UHPFRC Slabs under Blast Loads." In *Proceedings of Designing and Buildingwith UHPFRC: State-of-the-Art, Designing and Building with UHPFRC.*, edited by F Toutlemonde and J Resplendino, 363–76. Marseille, France: Wiley.

Schleyer, G K, S J Barnett, S G Millard, and G Wight. 2010. "Modelling the Response of UHPFRC Panels Toexplosive Loading." Edited by N JONES and U MANDER. *Structures Under Shock and Impact XI*, 2010.

Simula. 2016. "ABAQUS 6.14 User's Manual." Dassault Systèmes Simulia Corp.

Slotz, Alexander, Kai Fischer, Christoph Roller, and Stephan Hauser. 2014. "Dynamic Bearing Capacity of Ductile Concrete Plates under Blast Loading." *International Journal of Impact Engineering 69*, 25–38.

USACE, United States Army Corps of Engineers. 2017. "ConWep — PDC - Protective Design Center." 2017. https://pdc.usace.army.mil/software/conwep/.

Wahba, K., and H. Marzouk. 2012. "The Use of FBG Sensor to Determine The Fracture Energy Properties of UHPFRC." In *CSHM-4*. Berlin, Germany.

Wille, K, and A E Naaman. 2010. "Fracture Energy of UHPFRC under Direct Tensile Loading." In *FraMCoS-7 International Conference*. Jeju, Korea.

Xu, Man, and Kay Wille. 2015. "Fracture Energy of UHP-FRC under Direct Tensile Loading Appliedat Low Strain Rates." *Composites Part B: Engineering* 80: 116–25.

Yazidizadeh, Zahra. 2014. "Use of Fiber Brag Grating Sensors in Civil Engineering Appplications." *MASc., Thesis*. Toronto: Ryerson University.

Yi, Na-Hyun, Jang-Ho Jay Kim, Tong-Seok Han, Yun-Gu Cho, and Jang Hwa Lee. 2012. "Blast-Resistant Characteristics of Ultra-High Strength Concrete and Reactive Powder Concrete." *Construction and Building Materials* 28 (1): 694–707.

Yoo, Doo-Yeol Yoo, Nemkumar Banthia, and Youn Yoon. 2016. "Flexural Behavior of Ultra-High-Performance Fiber-Reinforced Concrete Beams Reinforced with GFRP and Steel Rebars." *Engineering Structures Journal.*